

553 Analyzing the uncertainty of estimating forest carbon stocks in

554 China

555 TianXiang Yue^{*1,2}, YiFu Wang^{1,2}, ZhengPing Du¹, MingWei Zhao^{1,2}, LiLi Zhang^{1,2},

556 Na Zhao¹, Ming Lu^{1,2}, Guy R. Larocque³, John P. Wilson^{1,4}

557

558 ¹State Key Laboratory of Resources and Environment Information System, Institute of

559 Geographical Science and Natural Resources Research

560 ²University of Chinese Academy of Sciences.

561 ³Natural Resources Canada, Canadian Forest Service, Laurentian Forestry Centre, 1055 du

562 P.E.P.S., G1V 4C7 Canada

563 ⁴Spatial Sciences Institute, Dana and David Dornsife College of Letters, Arts and Sciences,

564 University of Southern California

565

566

Corresponding author:

State Key Laboratory of Resources and Environment Information System, Institute of Geographical Science and Natural Resources Research, 11A, Datun Road, Anwai, Beijing 100101, China

* Email: yue@reis.ac.cn

567 **Abstract.** Earth surface systems are controlled by a combination of global and local factors,
568 which cannot be understood without accounting for both the local and global components.
569 The system dynamics cannot be recovered from the global or local controls alone. Ground
570 forest inventory is able to accurately estimate forest carbon stocks at sample plots, but these
571 sample plots are too sparse to support the spatial simulation of carbon stocks with required
572 accuracy. Satellite observation is an important source of global information for the simulation
573 of carbon stocks. Satellite remote-sensing can supply spatially continuous information about
574 the surface of forest carbon stocks, which is impossible from ground-based investigations, but
575 their description has considerable uncertainty. In this paper, we validated the Kriging method
576 for spatial interpolation of ground sample plots and a satellite-observation-based approach as
577 well as an approach for fusing the ground sample plots with satellite observations. The
578 validation results indicated that the data fusion approach reduced the uncertainty of estimating
579 carbon stocks. The data fusion had the lowest uncertainty by using an existing method for high
580 accuracy surface modeling to fuse the ground sample plots with the satellite observations
581 (HASM-SOA). The estimates produced with HASM-SOA were 26.1 and 28.4% more accurate
582 than the satellite-based approach and spatial interpolation of the sample plots, respectively. Forest
583 carbon stocks of 7.08 Pg were estimated for China during the period from 2004 to 2008, an
584 increase of 2.24 Pg from 1984 to 2008, using the preferred HASM-SOA method.

585

586 Key words

587 Satellite observation; Ground observation; Carbon stocks; HASM; Spatial interpolation; Data
588 fusion

589

590

591 **1 Introduction**

592 Biomass dynamics reflect the potential of vegetation to act as a carbon sink over the
593 long-term, as they integrate photosynthesis, autotrophic respiration and litter fall
594 fluxes (Thurner et al., 2014). Forest ecosystems cover more than 41 million km² of the
595 Earth's land surface and forests are thought to contain about half of the carbon in
596 terrestrial biomes (Prentice et al., 2001). Forests play an important role in the active
597 mitigation of atmospheric CO₂ through increased carbon stocks. The fixation of
598 atmospheric CO₂ into plant tissue through the process of photosynthesis is one of the
599 most effective mechanisms for offsetting carbon emissions (Canadell and Raupach,
600 2008; Gonzalez-Benecke et al., 2010).

601 Carbon sequestration by trees is the best way to store a large amount of terrestrial
602 carbon over long durations (Jung et al., 2013). Estimation of carbon stocks at scales
603 ranging from local to global is crucial for accurately predicting future changes in
604 atmospheric carbon dioxide (Yu et al., 2014). However, substantial uncertainties
605 remain in current model estimates of terrestrial carbon and there is an increasing need
606 to quantify and reduce these uncertainties (Barman et al., 2014; Ahlstrom et al.,
607 2012).

608 Several studies have estimated the forest carbon stocks in China. Piao et al.
609 (2005), for example, used a satellite-based approach and estimated that: (1) the total
610 forest biomass of China averaged 5.79 Pg C during the period 1981-1999, with an
611 average biomass density of 4.531 kg C m⁻²; and (2) the total forest biomass C stock
612 increased from 5.62 Pg C in the early 1980s to 5.99 Pg C by the end of the 1990s,
613 giving a total increase of 0.37 Pg C and an annual sequestration rate of 19 kg C yr⁻¹.
614 Zhang et al. (2007), on the other hand, analyzed seven forest inventories from 1973 to
615 2008 and suggested that the total biomass carbon stocks of all forest types increased

616 by 65% during this period, reaching 8.12 Pg C in 2008.

617 Wang et al. (2007) used the Integrated Terrestrial Ecosystem C-budget model and
618 estimated that China's forests were a source of 21.0 ± 7.8 Tg C yr⁻¹ due to human
619 activities during the period 1901-1949 and that this flux increased to 122.3 ± 25.3 Tg C
620 yr⁻¹ due to intensified human activities during the period 1950-1987. However, these
621 forests became large sinks of 176.7 ± 44.8 Tg C yr⁻¹ during the period 1988-2001
622 owing to large-scale plantation and forest regrowth in previously disturbed areas (see
623 the description of the Grain for Green Program below) as well as climatic warming,
624 atmospheric CO₂ fertilization, and N deposition.

625 Yang and Guan (2008), on the other hand, utilized the continuous Biomass
626 Expansion Factor (BEF) method with field measurements of forests plots in different
627 age classes and forest inventory data, and showed that the carbon density of the
628 forests in the Pearl River Delta increased by 14.3% from 19.08 to 21.81 kg C m⁻²
629 during the period 1989-2003. Similarly, Piao et al. (2009) reported that China's
630 terrestrial ecosystems were a net carbon sink of 0.19-0.26 Pg carbon per year and that
631 they absorbed 28-37% of the fossil carbon emissions during the 1980s and 1990s.
632 However, their results also showed that northeast China is a net source of CO₂ to the
633 atmosphere due to the over-harvesting and degradation of forests, while southern
634 China accounts for more than 65% of the carbon sink, which can be attributed to
635 regional climate change, large-scale plantation programs started in the 1980s, and
636 shrub recovery (Piao et al., 2009).

637 Guo et al. (2010) used three different approaches – the mean biomass density
638 (MBD) method, the mean ratio (MR) method, and the continuous BEF method (CBM)
639 – with forest inventory data to estimate China's forest biomass C stocks and their
640 changes from 1984 to 2003. The MBD, MR, and CBM estimated that forest biomass

641 C stocks increased from 5.7 to 7.7, 4.2 to 6.2, and 4.0 to 5.9 Pg C, respectively.

642 Deng et al. (2011) deployed a GIS approach and defined the vegetation carbon
643 sink as the carbon sequestration from the atmosphere ($1.63 \times \text{NPP}$), the vegetation
644 carbon stock as the carbon content that aboveground vegetation holds, and the soil
645 carbon stock as the carbon content that soil organic matter holds. These author's
646 estimated vegetation and soil carbon stocks of 1.58 and 1.41 Pg C, respectively in the
647 forest ecosystems of China for the period 1981-2000.

648 Ni (2013) used available national-scale information to estimate that: (1) the mean
649 vegetation carbon in China was 36.98 Pg and mean soil carbon was 100.75 Pg C; and
650 (2) that the forest and grassland sectors supported mean carbon stocks of 5.49 and
651 1.41 Pg C, respectively.

652 The aforementioned studies show that the forest ecosystems of China store
653 steadily increasing stocks of carbon and that these forest stands have great potential to
654 absorb more biomass carbon in the future due to large fractions of young and
655 middle-aged forests and programs to promote the conservation of soil and biological
656 resources.

657 All these published results relied on either ground- or satellite-observation-based
658 estimation unlike our own work in which we have tried to fuse these data sources to
659 reduce the uncertainty associated with the final carbon stock estimates.

660

661 **2. Data and Materials**

662 The forest distribution data were created by combining the Vegetation Map of the
663 People's Republic of China (Editorial Committee of Vegetation Map of China, 2007)
664 with a vegetation map produced from the forest inventory conducted during the period
665 from 2004 to 2008 (State Forestry Administration of China, 2009). The former

666 provides a detailed classification of plant functional types and describes the
667 phenological and regional character of forests in China, but it is not so exact. The
668 latter shows the forest distribution in the period of the forest inventory, but its
669 classification provides less information about plant functional types. The combination
670 of the two kinds of maps retains the the advantages of both.

671 The forest distribution data covers 161 plant biomes, including five classes of
672 deciduous needle-leaved trees, 57 classes of evergreen needle-leaved trees, 39 classes
673 of deciduous broad-leaved trees, 56 classes of evergreen broad-leaved trees and four
674 classes of mixed trees (Fig01).

675

676

Fig01

677

678 The national forestry inventory database (FID) for the period 2004-2008 includes
679 160,000 permanent sample plots and 90,000 temporary sample plots scattered across
680 China. The biomass density of each forest type in each province was calculated from
681 timber volume, using a BEF (Fang et al., 2007). The biomass carbon density (BCD)
682 of each forest type in each province was calculated next by multiplying the biomass
683 density by a carbon factor (CF) (Li and Lei, 2010). And finally, the biomass carbon
684 stock (BCS) of each forest type in each province was calculated by multiplying the
685 BCD by the area of that forest type. The total BCS in China is a sum of the BCS of all
686 of the forest types in the 31 provinces of China, excluding Taiwan, Hong Kong and
687 Macao.

688 The following formulations were used to calculate the forest BCS in China:

$$689 \quad TCS = \sum_{i=1}^M \sum_{j=1}^N (A_{i,j} \cdot BCD_{i,j}) \cdot 10^{-12} \quad (1)$$

$$690 \quad BCD_{i,j} = W_{i,j} \cdot CF_i \quad (2)$$

691 $W_{i,j} = BEF_i \cdot V_{i,j}$ (3)

692 $BEF_{i,j} = a_i + \frac{b_i}{V_{i,j}}$ (4)

693 where TCS is the total forest BCSs of China (Pg); $BCD_{i,j}$ is the area weighted
 694 biomass carbon density of the i th forest type in the j th province (kg/m^2); $A_{i,j}$ is the
 695 area of the i th forest type in the j th province (m^2); M and N refer to the numbers of
 696 forest types and provinces in China, respectively; $W_{i,j}$ is the area weighted mean
 697 forest biomass of the i th forest type in the j th province (kg/m^2); CF_i is the CF of the
 698 i th forest type; $V_{i,j}$ is the area weighted mean timber volume of the i th forest type in
 699 the j th province (m^3/m^2); BEF_i is the BEF of the i th forest type (kg/m^3); and a_i
 700 (kg/m^3) and b_i (kg/m^2) are constants of the i th forest type to be simulated. The mean
 701 CF_i of all coniferous forest types was used for coniferous mixed forest. The mean
 702 CF_i of all broad-leaved forest types was used for broad-leaved mixed forest. The
 703 mean CF_i of all broad-leaved and coniferous forest types was used for broad-leaved
 704 and coniferous mixed forest.

705 The land mass of China was next divided into nine regions (Fig02) with similar
 706 temperature, precipitation and soil regimes to make it easier to analyze changes in
 707 forest carbon storage from one place to another (Zhou et al., 1981). The nine regions
 708 are referred to as R_k where $k = 1$ to 9 and we use periods 1, 2, 3, 4 and 5 to
 709 represent the periods 1984-1988, 1989-1993, 1994-1998, 1999-2003 and 2004-2008,
 710 respectively.

711

712

Fig02

713

714

715 **3. Methods**

716 **3.1 Satellite-observation-based approach (SOA)**

717 The SOA used the normalized differential vegetation index (NDVI) at a temporal
718 resolution of one month and at a spatial resolution of 1 km x 1 km from the Earth
719 Observation System's moderate-resolution imaging spectroradiometer (EOS MODIS)
720 (Piao et al., 2009). The BCD from the FID data was matched with the NDVI data
721 through the map of forest in China reproduced in Fig01.

722 The BCD mirrored the latitude, longitude and maximum value of the
723 monthly-averaged NDVI values during the Seventh National Forest Inventory
724 conducted from 2004 to 2008:

$$725 \quad BCD_j = 93.351 \ln(NDVI_j) - 2.96 Lat_j - 21.388 Lon_j + 0.047 Lat_j^2 + 0.091 Lon_j^2 + 1339.03 \quad (5)$$

726 where $NDVI_j$ is the mean of the maximum values of the monthly-averaged NDVI
727 values during the period 2004-2008 in the j th province and Lat_j and Lon_j refer to
728 the latitude and longitude of the center of the j th province, respectively. The
729 coefficient of correlation ($R=0.91$) and significance ($P<0.001$) show how latitude,
730 longitude, and NDVI explained 83% of the variability in BCD.

731

732 **3.2 High accuracy surface modeling (HASM)**

733 HASM was developed for efficiently fusing satellite- with ground-observations to
734 find solutions for error problems which have long troubled earth surface modeling
735 (Yue, 2011). HASM has been successfully used to construct digital elevation models
736 (Yue et al. 2007, 2010a, 2010b; Yue and Wang, 2010; Chen and Yue 2010; Chen et al.
737 2013a, b), model surface soil properties (Shi et al. 2011) and soil pollution (Shi et al.

738 2009), fill voids in the Shuttle Radar Topography Mission (SRTM) dataset (Yue et al.
739 2012), simulate climate change (Yue et al. 2013a, b; Zhao and Yue 2014a, b), fill
740 voids in remotely sensed XCO₂ surfaces (Yue et al. 2015a), and to analyze ecosystem
741 responses to climatic change (Yue et al. 2015b). In all of these applications, HASM
742 produced more accurate results than the classical methods (Yue et al., 2015c).

743

744 **3.3 Estimation of carbon stocks**

745 Forest carbon stocks and carbon densities were estimated by methods of spatial
746 interpolation, SOA and data fusion. The spatial interpolation provided an effective
747 approach to construct a continuous surface from the FID by means of Kriging; it took
748 advantage of limited observation data to estimate the most plausible spatial
749 distribution by filling in missing data. The data fusion approach integrated the forest
750 inventory and satellite data into a consistent, accurate and useful representation using
751 HASM (HASM-SOA) (see supplement 1 in details); the aim of the data fusion was to
752 improve the quality of the information so that it was more accurate than would be
753 possible if the data sources had been used individually.

754

755 **3.4 Validation**

756 The uncertainties of the carbon stock estimates reported in earlier studies relied on
757 several different concepts and metrics. The same formula for absolute and relative
758 error should be used to evaluate all estimates of carbon stocks so that the estimation
759 results are comparable. We calculated the mean absolute errors (MAE) and mean
760 relative errors (MRE), respectively, as:

$$761 \quad MAE = \frac{1}{n} \sum_i^n |o_i - s_i| \quad (6)$$

762
$$MRE = \frac{MAE}{\frac{1}{n} \sum_i^n |o_i|} \quad (7)$$

763 where o_i represents the forest carbon stocks at the i th control point; s_i represents the
764 simulated value at the i th control point; and n_i is the total number of control points
765 used for validation.

766 **Cross-validation is used to estimate how accurately a model performs, which is**
767 **analyzed by removing certain data points in turn and summing the absolute value of**
768 **the discrepancy of each removed data point from the simulated one at the same**
769 **location (Hulme et al., 1995).** It was comprised of four steps: (1) 5 % of the sample
770 plots from the national forest inventory were removed for validation; (2) the spatial
771 distribution of average forest BCSs in China during the period 2004-2008 were
772 simulated at a spatial resolution of 5 km × 5 km using the remaining 95% of the
773 sample plots from the national forest inventory by means of the different methods; (3)
774 the MAEs and MREs were calculated using the 5% validation set; and (4) the 5%
775 validation set was returned to the pool for the next iteration, and another 5%
776 validation set was removed. This final process was repeated until all the sample plots
777 were used for validation at least one time and the simulation error statistics could be
778 calculated for each sample plot.

779

780 **4 Results**

781 The three maps of mean annual carbon stocks during the period 2004-2008
782 reproduced with each of the aforementioned methods shows how each of the methods
783 was able to generate the same overall patterns based on the underlying forest cover on
784 the one hand, and how the estimates varied using each of these methods over large
785 parts of the China on the other hand (Fig03). This variability raises questions related

786 to the reliability of the estimates produced with the three aforementioned approaches.

787

788

Fig03

789

790 The cross-validation results indicated that Kriging and SOA had larger errors, with
791 MREs of 50.12 and 48.77%, respectively. Kriging over-estimated the carbon stocks,
792 while SOA under-estimated the carbon stocks (Table 1). Accuracy was considerably
793 improved when the forest inventory and satellite data were fused by using
794 HASM-SOA. The MRE of HASM-SOA was 22.71%.

795

796 **Table 1**

797

798 The BCSs of all forest types estimated with HASM-SOA (the best approach) was
799 7.08 Pg in China during the period 2004-2008. The BCSs of coniferous, broadleaf and
800 mixed forests were 2.74, 3.95 and 0.39 Pg, respectively (Table 1). The mean carbon
801 densities (MBCDs) of the coniferous, broadleaf and mixed forests were 4.35, 4.74 and
802 4.20 kg/m², respectively.

803 The HASM-SOA estimates showed that 89.9% of the MBCSs were found in the
804 regions R5, R3, R6, R9 and R7 during the period P5, accounting for 28.61, 28.41,
805 14.48, 12.52 and 5.89% of the BCSs, respectively. The three largest BCDs occurred in
806 R5 (Tibet plateau; 10.53 kg/m²), R2 (arid area; 6.33 kg/m²) and R3 (northeastern
807 China; 4.44 kg/m²) (Table 2 and Fig03c). The two smallest BCDs were predicted in
808 the R8 (2.14 kg/m²) and R9 (2.60 kg/m²) regions.

809

810 **Table 2**

811

812 The HASM-SOA estimates can be parsed by forest type as well (Table 3). Hence,
813 the BCDs of evergreen broad-leaved and evergreen coniferous forests were 6.23 and
814 4.47 kg/m², respectively, while the BCDs for deciduous broad-leaved and deciduous
815 coniferous forests were 3.93 and 3.77 kg/m², respectively in P5. The BCD of
816 evergreen forests was 50% larger than that of deciduous forests, and the BCDs for
817 broad-leaved forests were greater than those for both coniferous and deciduous forests.
818 Turning next to the BCSs, the evergreen coniferous forests contributed the largest
819 proportion, accounting for 33.05%, followed by deciduous broad-leaved forests
820 (29.8%), and evergreen broad-leaved forests (25.99%). The deciduous coniferous and
821 the broad-leaved and coniferous mixed forests accounted for the first two smallest
822 proportions of the total BCS, 5.65 and 5.51%, respectively.

823

824 **Table 3**

825

826 The HASM-SOA estimates also indicate that BCSs rose from 4.84 Pg in period 1
827 to 7.08 Pg in P5 due to the increase of BCD and the expansion of forest area (Table 4).
828 The BCD rose from 4.00 kg/m² in P1 to 4.55 kg/m² in P5 and the forest area grew
829 from 1.21 million km² in P1 to 1.56 million km² in P5. The increasing trends of the
830 BCS, BCD and forest area (FA) are captured by the following regression equations:

$$831 \quad BCS(t) = 0.531t + 4.297 \quad R = 0.976 \quad (8)$$

$$832 \quad BCD(t) = 0.125t + 3.958 \quad R = 0.943 \quad (9)$$

$$833 \quad FA(t) = 0.083t + 1.1045 \quad R = 0.96 \quad (10)$$

834 where t corresponds to periods 1, 2, 3, 4 and 5; $BCS(t)$, $BCD(t)$ and $FA(t)$ are
835 BCS, BCD and FA, respectively in the period t ; and R represents the correlation
836 coefficient for the corresponding regression equation.

837

838 **Table 4**

839

840 Although BCS rose in all nine regions from period 1 to period 5, the spatial
841 variability over China more or less mirrors the variability in the distribution of forests
842 (Fig04, Fig05, Table 4). For regions R1 and R8, for example, both BCS and BCD
843 have continuously increased from period 1 to period 5. R8 has the smallest BCS,
844 which only accounted for 0.83% of the BCS of the whole of China, and the smallest
845 BCD of 2.14 kg/m^2 in P5 as well as the lowest BCS accumulation rate of 1.3 Tg yr^{-1} .
846 In R1, BCS accounted for 3.94% of the total BCS of China for the period of P5 and
847 the BCS accumulation rate has averaged 6.2 Tg yr^{-1} from P1 to P5.

848

849 **Fig04**

850

851 **Fig05**

852

853 The region R5 had the largest BCS accounting for 28.61% of the total BCS of
854 China in P5, the largest BCD of 10.53 kg/m^2 and the fastest BCS accumulation rate of
855 52 Tg yr^{-1} ; the BCS has shown a monotonically increasing trend since P1. The second
856 largest BCS occurred in R3 (Northeastern China). The BCS in R3 accounted for 28.41%
857 of the total BCS of China. However, the BCD in R3 has declined since P3 following
858 increases from P1 to P2 and from P2 to P3. The mean BCS accumulation rate in R3
859 was 21.3 Tg/yr .

860 In the regions R4 (Loess Plateau), R6 and R9, both BCS and BCD have increased
861 since P3. The BCSs in R4, R6 and R9 accounted for 2.68, 14.48 and 12.26% of the
862 BCS in the whole of China in P5, respectively. The average BCS accumulation rates
863 were 2.8, 10.4 and 12.7 Tg yr^{-1} , respectively in R4, R6, and R9. In R2 (an arid area of

864 China), the BCS accounted for 2.80% of the total for China in the period P5. The BCS
865 and BCD increased from P4 to P5, but the mean accumulation rate of BCS was only
866 2.3 Tg yr^{-1} . The BCS accounted for 5.89% of the total for China in R7. The BCS and
867 BCD both increased from P4 to P5 but like in R2, the mean BCS accumulation rate
868 was relatively low at just 2.9 Pg yr^{-1} .

869 In terms of forest types, evergreen broad-leaved forests had the fastest BCS
870 accumulation rate and the largest BCD, while evergreen coniferous forests contributed
871 the largest BCS. The BCSs of broad-leaved forests increased during all five periods.
872 The BCS of evergreen broad-leaved forests increased from 0.63 Pg in period 1 to 1.84
873 Pg in period 5, and the BCSs for deciduous broad-leaved forests rose from 1.38 Pg in
874 period 1 to 2.11 Pg in period 5. These trends can be modeled with the following
875 regression equations:

$$876 \quad BCS_1(t) = 0.312t + 0.286, \quad R = 0.998 \quad (11)$$

$$877 \quad BCS_2(t) = 0.199t + 1.115, \quad R = 0.981 \quad (12)$$

878 where t corresponds to period t , $t = 1, 2, 3, 4$ and 5 ; $BCS_1(t)$ and $BCS_2(t)$ are
879 respectively the BCSs of evergreen broad-leaved forests and deciduous broad-leaved
880 forests in the period t and R represents the correlation coefficient of the
881 corresponding regression equation.

882 The BCSs of deciduous coniferous forests fluctuated from period to period.
883 Evergreen coniferous forests and broad-leaved and coniferous mixed forests exhibited
884 an increasing trend of BCS in general but declined in period 3. Their trends were
885 modeled with the following regression equations:

$$886 \quad BCS_3(t) = 0.207t + 1.391, \quad R = 0.932 \quad (13)$$

$$887 \quad BCS_4(t) = 0.076t - 0.068, \quad R = 0.867 \quad (14)$$

888 where t corresponds to periods 1, 2, 3, 4 and 5; $BCS_3(t)$ represents the BCSs of
889 evergreen coniferous forests in the period t ; $BCS_4(t)$ refers to the broad-leaved and
890 coniferous mixed forests; and R represents the correlation coefficient of the
891 corresponding regression equation.

892 The equations (8), (9) and (10) indicate that increasing rates of BCS, BCD and
893 FA were 0.531 Pg, 0.125 kg/ m² and 0.083 million km², respectively over a five-year
894 period on average. According to equations (11) and (12), the BCS of evergreen
895 broad-leaved forests had a growth rate of 0.312 Pg over a five-year period, which was
896 0.113 Pg higher than that for deciduous broad-leaved forests because of the different
897 increasing rates of BCD; the BCD of evergreen broad-leaved forests increased by 1.87
898 kg/m², while the BCD of deciduous broad-leaved forests increased by 0.18 kg/m²
899 from period 1 to period 5. The equations (13) and (14) show that carbon stocks of
900 evergreen coniferous forests grew much faster than those for broad-leaved and
901 coniferous mixed forests. The former grew by 0.207 Pg but the latter by only 0.076 Pg
902 in a five-year period on average because the area of evergreen coniferous forests was
903 five times larger (0.50×10^6 km² compared to 0.09×10^6 km² for broad-leaved and
904 coniferous mixed forests) and offset the lower BCD growth rate of the former (0.132
905 kg/m²) compared to 0.56 kg/m² for broad-leaved and coniferous mixed forests per
906 five-year period.

907 The results from Kriging and HASM-SOA exhibit a similar spatial pattern on the
908 national level, especially in southern Tibet, the Xiao Hinggan Moutains, the Changbai
909 Mountains, and south China. Some differences occur in Taiwan and Xinjiang as well
910 as the Qinling Mountains. Compared to HASM-SOA, Kriging is strongly influenced
911 by sample-plot density. The spatial heterogeneity of the results from SOA is not so
912 obvious because NDVI, a critical variable of SOA, is not so sensitive to a change of

913 carbon stocks, especially in northeast China and the lower reaches of Yangtze River.

914 The scatter diagrams of simulated BCD against observed BCD (Fig06) indicate
915 that the BCD surface created by Kriging exhibits a higher correlation with observed
916 BCD, $R^2=0.826$. But the Kriging interpolation generated large errors in the
917 Xizang/Tibet and Xinjing regions, with the highest BCD. The BCD was
918 overestimated in Xizang and underestimated in Xinjiang. The BCD surface created by
919 SOA has the smallest correlation coefficient, $R^2= 0.627$, with the observed one. The
920 SOA results show that BCDs in higher and lower latitudes are larger than those in
921 middle latitudes, but for Xinjiang and Xizang. The BCD was overestimated in
922 Xinjiang but underestimated in Xizang. The surface of BCDs generated by
923 HASM-SOA has the best correlation with the observed one, $R^2=0.943$ and it
924 generated the smallest errors in the regions of Xizang and Xinjiang, compared with
925 the other methods.

926

927 Fig06

928

929

930 **5 Discussion and Conclusions**

931 The fusion of forest inventory data with satellite observations achieved with
932 HASM-SOA provided much more accurate estimates of forest biomass carbon stocks
933 and their changes. This kind of method can increase our understanding of the role of
934 forests in the carbon cycle, for greenhouse gas inventories, and terrestrial carbon
935 accounting (Muukkonen and Heiskanen, 2007).

936 Turning to the work at hand, HASM-SOA overcame the shortcomings of both the
937 ground-based national forest inventory and the satellite remote-sensing observations

938 by fusing information about the details of the carbon stocks observed on the Earth's
939 surface and the variability of the carbon surface observed from space. The
940 cross-validation demonstrated that HASM-SOA was 26.1% more accurate than the
941 satellite-based approach and 28.4% more accurate than spatial interpolation of the
942 sample plots. These findings suggest that China's forest biomass carbon stocks are
943 more likely to match our estimates than those generated by past efforts to estimate
944 these same carbon stocks and their change over time.

945 Taken as a whole, the HASM-SOA results show that the forest carbon stocks of
946 China have increased by 2.24 Pg during the period 1984-2008 to a new high of 7.08
947 Pg C in 2008. These numbers fall in the middle of the previously published estimates.
948 All of the estimates show forest biomass carbon stocks in China increasing from 1973
949 to 2008, notwithstanding the various methods used and the varying levels of
950 uncertainty embedded in these different methods and the data sources used.

951 The results from HASM-SOA are more or less different from those of other
952 studies. For instance, the annual growth of total BCS from period 1 (circa 1986) to
953 period 5 (circa 2006) in China was 0.112 PgCyr^{-1} . This estimate was higher than that
954 of Zhang et al. (2013), which was 0.103 PgCyr^{-1} . However, our estimate of 0.148
955 PgCyr^{-1} from period 3 (circa 1996) to period 5 (circa 2006) - was lower than the 0.174
956 PgCyr^{-1} estimated by Zhang et al. (2013). From period 4 (circa 2001) to period 5
957 (circa 2006), the 0.14 PgCyr^{-1} estimated by HASM-SOA was twice that estimated by
958 Liu et al. (2015).

959 The Grain for Green program, which was launched in 1999 and aims to restore
960 the country's forests and grasslands to prevent soil erosion, has emerged as one of the
961 key drivers of carbon sequestration. This program targets land with slopes $> 25^\circ$ (Xu
962 et al., 2006; Yue et al., 2010c) and has been implemented in four phases: (1) a pilot

963 phase (1999-2001); (2) an initial construction phase (2002-2010); (3) a consolidation
964 phase (2011-2013); and (4) a second construction phase to be built around a new
965 round of Grain for Green program expenditures (2014-2020).

966 The pilot program launched in 1999 focused on three provinces: Gansu, Shaanxi
967 and Sichuan. Approximately 381,000 ha of farmland was converted into forestland
968 and 66,000 ha of bare land was reforested. In 2000, the program was expanded to 17
969 provinces, and the converted farmland and reforested bare land totals grew to 410,000
970 and 449,000 ha, respectively. By 2001, 20 provinces were involved in the program
971 and 420,000 and 563,000 ha of farm and bare land had been reforested, respectively
972 (Table 5). The national Grain for Green program was launched in China in 2002 and
973 by the end of 2010, 14.667 million ha of farmland had been converted to forest or
974 grassland and 17.333 million ha of bare land had been reforested. During the
975 consolidation phase from 2011 to 2013, scientific monitoring and management of the
976 converted and reforested lands was strengthened to sustain the aforementioned
977 achievements of the Grain for Green program over the long-term.

978

979 **Table 5**

980

981 To grow and consolidate these gains, the potential for farmland conversion at the
982 county level during the period 2014-2020 was estimated in 2014 by counting up
983 farmers' voluntary applications to determine how large an area could be converted to
984 forest or grassland. By 2020, 2.827 million ha of farmland could be converted, which
985 includes 1.449 million ha of farmland with slopes $>25^\circ$, 1.133 million ha of cultivated
986 land threatened by desertification, and 247,000 ha of farmland with slopes between 15
987 and 25° around the Danjiangkou and Three Gorges reservoirs.

988 The results from this latest phase of the Grain for Green program are encouraging.
989 Participating farmers can choose whether farmland is to be converted to forest or
990 grassland, and which species will be planted, and they will receive a 22,500 RMB
991 subsidy for every hectare of farmland converted to forest or grassland. In 2014,
992 322,000 ha were converted to forest and 11,000 ha were converted to grassland, and
993 in 2015 another 667,000 ha of farmland will be converted to either forest or grassland.

994 The BCS growth was contributed by already existing forests and newly planted
995 forests. The former accounted for about 55% while the latter about 40%. The BCS in
996 existing forests had a growth rate of about 0.55 kg/m² per five-year period and the
997 BCS in newly planted forests grew at 1.8 kg/m² per five-year period.

998

999 *Acknowledgments.* This work was supported by the National Natural Science
1000 Foundation of China (91325204), by the National High-tech R&D Program of the
1001 Ministry of Science and Technology of the People's Republic of China
1002 (2013AA122003), and by the National Basic Research Priorities Program
1003 (2010CB950904) of the Ministry of Science and Technology of the People's Republic
1004 of China.

1005

1006 **References**

1007 Ahlstrom, A., Schurgers, G., Arneeth, A. and Smith, B.: Robustness and uncertainty
1008 in terrestrial ecosystem carbon response to CMIP5 climate change projections,
1009 Environmental Research Letters, 7, 044008, 2012.

1010 Barman, R., Jain, A.K. and Liang, M.L.: Climate-driven uncertainties in modeling
1011 terrestrial gross primary production: A site level to global-scale analysis, Global
1012 Change Biology, 20, 1394-1411, 2014.

1013 Canadell, J.G. and Raupach, M.R.: Managing forests for climate change mitigation,
1014 Science, 320, 1456-457, 2008.

1015 Chen, C.F., Li, Y.Y. and Yue, T.X.: Surface modeling of DEMs based on a sequential
1016 adjustment method, International Journal of Geographical Information Science,
1017 27, 1272-1291, 2013b.

1018 Chen, C.F., Yue, T.X., Dai, H.L. and Tian, M.Y.: The smoothness of HASM,
1019 International Journal of Geographical Information Science 27, 1651-1667, 2013a.

1020 Deng, S.H., Shi, Y.Q., Jin, Y. and Wang, L.H.: A GIS-based approach for quantifying
1021 and mapping carbon sink and stock values of forest ecosystem: A case study,
1022 Energy Procedia, 5, 1535-1545, 2011.

1023 Editorial Committee of Vegetation Map of China: Vegetation Map of the People's
1024 Republic of China. Geological Publishing House, Beijing, 2007 (in Chinese).

1025 Gonzalez-Benecke, C.A., Martin, T.A., Cropper Jr., W.P. and Bracho, R.: Forest
1026 management effects on in situ and ex situ slash pine forest carbon balance, Forest
1027 Ecology and Management, 260, 795-805, 2010.

1028 Guo, Z.D., Fang, J.Y., Pan, Y.D. and Birdsey, R.: Inventory-based estimates of forest
1029 biomass carbon stocks in China: A comparison of three methods, Forest Ecology
1030 and Management, 259, 1225-1231, 2010.

1031 Hulme, M., Conway, D., Jones, P.D., Jiang, T., Barrow, E.M., Turney, C.: Construction
1032 of a 1961-1990 European climatology for climate change modelling and impact
1033 applications, International Journal of Climatology 15, 1333-1363, 1995.

1034 Jung, J., Kim, S., Hong, S., Kim, K., Kim, E., Im, J. and Heo, J.: Effects of national
1035 forest inventory plot location error on forest carbon stock estimation using
1036 k-nearest neighbor algorithm, ISPRS Journal of Photogrammetry and Remote
1037 Sensing, 81, 82-92, 2013.

1038 Li, H.K. and Lei, Y.C.: Estimation and Evaluation of Forest Biomass Carbon Storage
1039 in China, China Forestry Press (in Chinese), Beijing, 2010.

1040 Liu, Y.Y., van Dijk, A.I.J.M., de Jeu, R.A.M., Canadell, J.G., McCabe, M.F., Evans,
1041 J.P., Wang, G.J.: Recent reversal in loss of global terrestrial biomass. *Nature*
1042 *Climate Change*, DOI: 10.1038/NCLIMATE2581, 2015.

1043 Muukkonen, P. and Heiskanen, J.: Biomass estimation over a large area based on
1044 standwise forest inventory data and ASTER and MODIS satellite data: A
1045 possibility to verify carbon inventories, *Remote Sensing of Environment*, 107,
1046 617-624, 2007.

1047 Office of Converting Farmland to Forestry, State Forestry Administration of China: A
1048 new round of the overall concept of returning farmland to forest and grass,
1049 *Newsletter for Converting Farmland to Forestry*, 194, 1-2, 2014 (in Chinese).

1050 Office of Converting Farmland to Forestry, State Forestry Administration of China:
1051 *New Year's Speech*, *Newsletter for Converting Farmland to Forestry*, 198, 1-2,
1052 2016 (in Chinese).

1053 Piao, S.L., Fang, J.Y., Ciais, P., Peylin, P., Huang, Y., Sitch, S. and Wang, T.: The
1054 carbon balance of terrestrial ecosystems in China, *Nature*, 458, 1009-1014, 2009.

1055 Piao, S.L., Fang, J.Y., Zhu, B. and Tan, K.: Forest biomass carbon stocks in China
1056 over the past 2 decades: Estimation based on integrated inventory and satellite
1057 data, *Journal of Geophysical Research*, 110, G01006, 2005.

1058 Prentice, I.C., Farquhar, G.D., Fasham, M.J.R., Goulden, M.L., Heimann, M.,
1059 Jaramillo, V.J., Kheshgi, H.S., Le Quere, C., Scholes, R.J., Wallace, D.W.R.,
1060 Archer, D., Ashmore, M.R., Aumont, O., Baker, D., Battle, M., Bender, M., Bopp,
1061 L.P., Bousquet, P., Caldeira, K., Ciais, P., Cox, P.M., Cramer, W., Dentener, F.,
1062 Enting, I.G., Field, C.B., Friedlingstein, P., Holland, E.A., Houghton, R.A.,

1063 House, J.I., Ishida, A., Jain, A.K., Janssens, I.A., Joos, F., Kaminski, T., Keeling,
1064 C.D., Keeling, R.F., Kicklighter, D.W., Hohfeld, K.E., Knorr, W., Law, R.,
1065 Lenton, T., Lindsay, K., Maier-Reimer, E., Manning, A.C., Matear, R.J.,
1066 McGuire, A.D., Melillo, J.M., Meyer, R., Mund, M., Orr, J.C., Piper, S., Plattner,
1067 K., Rayner, P.J., Sitch, S., Slater, R., Taguchi, S., Tans, P.P., Tian, H.Q., Weirig,
1068 M.F., Whorf, T. and Yool, A.: The carbon cycle and atmospheric carbon dioxide.
1069 In Houghton, J.T., Ding, Y., Griggs, D.J., Noguer, M., Van Der Linden, P.J., Dai,
1070 X., Maskell, K., Johnson, C.A. (Eds.) *Climate Change 2001: The Scientific Basis*.
1071 Cambridge, Cambridge University Press, 183-237, 2001.

1072 Shi, W.J., Liu, J.Y., Song, Y.J., Du, Z.P., Chen, C.F. and Yue, T.X.: Surface modeling
1073 of soil pH, *Geoderma*, 150, 113-119, 2009.

1074 *State Forestry Administration of China: National Forest Report (2004-2008), China*
1075 *Forestry Publishing House, Beijing, 2009 (in Chinese)*.

1076 Thurner, M., Beer, C., Santoro, M., Carvalhais, N., Wutzler, T., Schepaschenko, D.,
1077 Shvidenko, A., Kompter, E., Ahrens, B., Levick, S.R. and Schullius, C.: Carbon
1078 stock and density of northern boreal and temperate forests, *Global Ecology and*
1079 *Biogeography*, 23, 297-310, 2014.

1080 Wang, S., Chen, J.M., Ju, W.M., Feng, X., Chen, M., Chen, P. and Yu, G.: Carbon
1081 sinks and sources in China's forests during 1901-2001, *Journal of Environmental*
1082 *Management*, 85, 524-537, 2007.

1083 Xu, Z.G., Xu, J.T., Deng, X.Z., Huang, J.K., Uchida, E. and Rozelle, S.: Grain for Green
1084 versus grain: Conflict between food security and conservation set-aside in China,
1085 *World Development*, 34, 130-148, 2006.

1086 Yang, K. and Guan, D.S.: Changes in forest biomass carbon stock in the Pearl River
1087 Delta between 1989 and 2003, *Journal of Environmental Sciences*, 20, 1439-1444,

1088 2008.

1089 Yu, G.R., Chen, Z., Piao, S.L., Peng, C.H., Ciais, P., Wang, Q.F., Li, X.R. and Zhu,
1090 X.J.: High carbon dioxide uptake by subtropical forest ecosystems in the East
1091 Asian monsoon region, Proceedings of the National Academy of the Sciences of
1092 the USA, 111, 4910-4915, 2014.

1093 **Yue, T.X., Chen, C.F., Li, B.L.: A high accuracy method for filling SRTM voids and
1094 its verification. International Journal of Remote Sensing, 33(9), 2815-2830, 2012.**

1095 Yue, T.X., Liu, Y., Zhao, M.W., Du, Z.P., Zhao, N.: A fundamental theorem of
1096 Earth's surface modelling. Environmental Earth Sciences, (in press), 2016.

1097 Yue, T.X., Du, Z.P., Lu, M., Fan, Z.M., Wang, C.L., Tian, Y.Z. and Xu, B.: Surface
1098 modelling of ecosystem responses to climatic change, Ecological Modelling, 306,
1099 16-23, 2015a.

1100 Yue, T.X., Zhao, M.W. and Zhang, X.Y.: A high-accuracy method for filling voids on
1101 remotely sensed XCO₂ surfaces and its verification, Journal of Cleaner
1102 Production, 103, 819-827, 2015b.

1103 Yue, T.X., Zhang, L.L., Zhao, N., Zhao, M.W., Chen, C.F., Du, Z.P., Song, D.J., Fan,
1104 Z.M., Shi, W.J., Wang, S.H., Yan, C.Q., Li, Q.Q., Sun, X.F., Yang, H., Wang,
1105 C.L., Wang, Y.F., Wilson, J.P., and Xu, B.: A review of recent developments in
1106 HASM, Environmental Earth Sciences, 74(8), 6541-6549, 2015c.

1107 Yue, T.X., Zhao, N., Yang, H., Song, Y.J., Du, Z.P., Fan, Z.M. and Song, D.J.: The
1108 multi-grid method of high accuracy surface modelling and its validation,
1109 Transactions in GIS, 17, 943-952, 2013a.

1110 Yue, T.X., Zhao, N., Ramsey, R.D., Wang, C.L., Fan, Z.M., Chen, C.F., Lu, Y.M. and
1111 Li, B.L.: Climate change trend in China, with improved accuracy, Climate
1112 Change, 120, 137-151, 2013b.

1113 Yue, T.X., Chen, C.F. and Li, B.L.: A high accuracy method for filling SRTM voids
1114 and its verification, *International Journal of Remote Sensing*, 33, 2815–2830,
1115 2012.

1116 Yue, T.X.: *Surface Modelling: High Accuracy and High Speed Methods*, CRC Press,
1117 Boca Raton, FL, 2011.

1118 Yue, T.X., Chen, C.F. and Li, B.L.: An adaptive method of high accuracy surface
1119 modeling and its application to simulating elevation surfaces, *Transactions in GIS*,
1120 14, 615-630, 2010a.

1121 Yue, T.X., Song, D.J., Du, Z.P. and Wang, W.: High-accuracy surface modelling and
1122 its application to DEM generation, *International Journal of Remote Sensing*, 31,
1123 2205-2226, 2010b.

1124 Yue, T.X. and Wang, S.H.: Adjustment computation of HASM: A high-accuracy and
1125 high-speed method, *International Journal of Geographical Information Science*,
1126 24, 1725–1743, 2010.

1127 Yue, T.X., Wang, Q., Lu, Y.M., Xin, X.P., Zhang, H.B. and Wu, S.X.: Change trends
1128 of food provisions in China, *Global and Planetary Change*, 72(3), 118-130,
1129 2010c.

1130 Yue, T.X., Du, Z.P., Song, D.J. and Gong, Y.: A new method of surface modeling and
1131 its application to DEM construction, *Geomorphology*, 91, 161-172, 2007.

1132 Zhang, C.H., Ju, W.M., Chen, J.M., Zan, M., Li, D.Q., Zhou, Y.L. and Wang, X.Q.:
1133 China's forest biomass carbon sink based on seven inventories from 1973 to 2008,
1134 *Climatic Change*, 118, 933-948, 2013.

1135 Zhao, N. and Yue, T.X.: A modification of HASM for interpolating precipitation in
1136 China, *Theoretical and Applied Climatology*, 116, 273-285, 2014a.

1137 Zhao, N. and Yue, T.X.: Sensitivity studies of a high accuracy surface modelling

- 1138 method, *Science China-Earth Science*, 57, 1-11, 2014b.
- 1139 Zhou, L.S., Sun, H., Shen, Y.Q., Deng, J.Z., Shi, Y.L.: *Comprehensive Agricultural*
- 1140 *Planning of China*, China Agricultural Press, Beijing (in Chinese), 1981.
- 1141
- 1142
- 1143
- 1144
- 1145
- 1146
- 1147
- 1148
- 1149
- 1150
- 1151
- 1152
- 1153
- 1154
- 1155
- 1156
- 1157
- 1158
- 1159
- 1160
- 1161
- 1162

1163

1164 **Table 1. Biomass carbon stocks and biomass carbon densities as well as their errors produced by different**
1165 **methods.**

Method	Calculated object	Coniferous forests	Mixed forests	Broadleaf forests	Total	MAE (kg m ⁻²)	MRE (%)
SOA	BCS (Pg)	2.48	0.46	3.61	6.55	1.92	48.77
	BCD (kg m ⁻²)	3.94	4.93	4.34			
Kriging	BCS (Pg)	2.76	0.39	4.11	7.26	1.97	50.12
	BCD (kg m ⁻²)	4.38	4.24	4.94			
HASM-SOA	BCS (Pg)	2.74	0.39	3.95	7.08	0.89	22.71
	BCD (kg m ⁻²)	4.35	4.2	4.74			

1166

1167

1168

1169

1170

1171

1172

1173

1174

1175

1176

1177

1178

1179

1180

1181

1182

1183 Table 2. BCS and BCD of the forests in the nine regions of China during the periods 2004-2008 and
 1184 1984-1988

Regions	P5 (from 2004 to 2008)			P1 (from 1984 to 1988)		BCS accumulation rate (Tg yr ⁻¹)
	BCD kg m ⁻²	BCS (Pg)	Percentage (%)	BCD kg m ⁻²	BCS (Pg)	
R1	3.710	0.28	3.94	2.666	0.16	6.2
R2	6.330	0.20	2.80	6.358	0.15	2.3
R3	4.445	2.01	28.41	4.493	1.59	21.3
R4	3.274	0.19	2.68	3.035	0.13	2.8
R5	10.525	2.03	28.61	6.718	0.99	52.0
R6	3.671	1.03	14.48	3.734	0.82	10.4
R7	3.693	0.42	5.89	3.643	0.36	2.9
R8	2.138	0.06	0.83	1.515	0.03	1.3
R9	2.598	0.87	12.26	2.358	0.62	12.7
Total		7.08	100		4.84	112

1185
 1186
 1187
 1188
 1189
 1190
 1191
 1192
 1193
 1194
 1195
 1196
 1197
 1198
 1199
 1200
 1201
 1202
 1203

1204 **Table 3. BCSs and BCDs for all forest types during the five periods estimated using HASM-SOA**

Period	Calculation object	Deciduous coniferous forests	Evergreen coniferous forests	Broad-leaved and coniferous mixed forests	Deciduous broad-leaved forests	Evergreen broad-leaved forests
P1	BCS (Pg)	0.41	1.50	0.06	1.38	0.63
	BCD (kg/m²)	4.35	3.81	3.08	3.75	4.35
P2	BCS (Pg)	0.39	1.80	0.09	1.44	0.87
	BCD (kg/m²)	4.28	4.13	3.75	3.77	5.65
P3	BCS (Pg)	0.44	2.23	0.07	1.66	1.20
	BCD (kg/m²)	4.20	4.09	3.03	3.87	6.35
P4	BCS (Pg)	0.47	2.19	0.19	1.97	1.57
	BCD (kg/m²)	4.37	4.40	5.18	3.89	7.49
P5	BCS (Pg)	0.40	2.34	0.39	2.11	1.84
	BCD (kg/m²)	3.77	4.47	4.20	3.93	6.22

1205

1206

1207

1208

1209

1210

1211

1212

1213

1214

1215

1216

1217

1218

1219

1220 **Table 4 Biomass carbon stocks and biomass carbon densities estimated by HASM-SOA**

Regions	Calculation object	Period 1	Period 2	Period 3	Period 4	Period 5
R1	BCS (Pg)	0.16	0.17	0.17	0.2	0.28
	BCD (kg m ⁻²)	2.67	2.71	2.88	2.98	3.71
R2	BCS (Pg)	0.15	0.16	0.15	0.18	0.2
	BCD (kg m ⁻²)	6.36	6.27	6.25	6.23	6.33
R3	BCS (Pg)	1.59	1.64	1.64	1.77	2.01
	BCD (kg m ⁻²)	4.49	4.42	4.5	4.43	4.44
R4	BCS (Pg)	0.13	0.15	0.14	0.16	0.19
	BCD (kg m ⁻²)	3.04	3.23	3.13	3.15	3.27
R5	BCS (Pg)	0.99	1.57	1.64	1.94	2.03
	BCD (kg m ⁻²)	6.72	10.15	10.83	11.49	10.53
R6	BCS (Pg)	0.82	0.87	0.82	0.96	1.03
	BCD (kg m ⁻²)	3.73	3.78	3.66	3.88	3.67
R7	BCS (Pg)	0.36	0.39	0.37	0.4	0.42
	BCD (kg m ⁻²)	3.64	3.79	3.66	3.54	3.69
R8	BCS (Pg)	0.03	0.04	0.04	0.05	0.06
	BCD (kg m ⁻²)	1.52	1.64	1.89	1.89	2.14
R9	BCS (Pg)	0.62	0.56	0.62	0.73	0.87
	BCD (kg m ⁻²)	2.36	2.05	2.3	2.51	2.6
The whole of China	BCS (Pg)	4.84	5.55	5.6	6.38	7.08
	BCD (kg m ⁻²)	4	4.32	4.33	4.47	4.55
	Area (million km ²)	1.2101	1.2864	1.292	1.4279	1.5559

1221

1222

1223

1224

1225

1226

1227

1228

1229 **Table 5. Converted farmland and reforested bare land included in China's Grain for Green Program**
 1230 **(millions hectares) (Office of Converting Farmland to Forestry, State Forestry Administration of China,**
 1231 **2014, 2016)**

Year	Converted farmland	Afforestation on bare land	Total
1999	0.381	0.066	0.448
2000	0.405	0.468	0.872
2001	0.42	0.563	0.983
2002	2.647	3.082	5.729
2003	3.367	3.767	7.133
2004	0.667	3.333	4
2005	1.114	1.321	2.435
2006-2010	5.666	4.733	10.4
2014	0.333		0.333
2015	0.667		0.667
1999-2015	15.667	17.333	33
2016-2020	1.827		1.827

1232
 1233
 1234
 1235
 1236
 1237
 1238
 1239
 1240
 1241
 1242
 1243
 1244
 1245

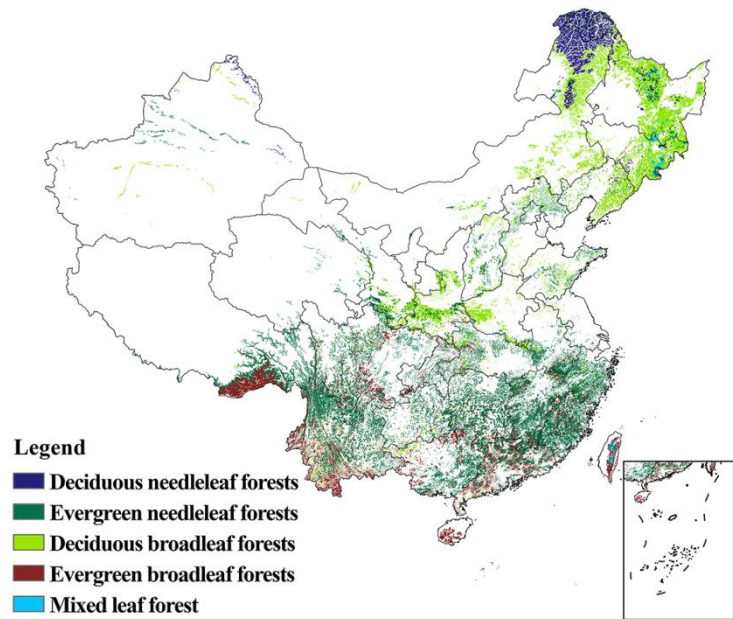
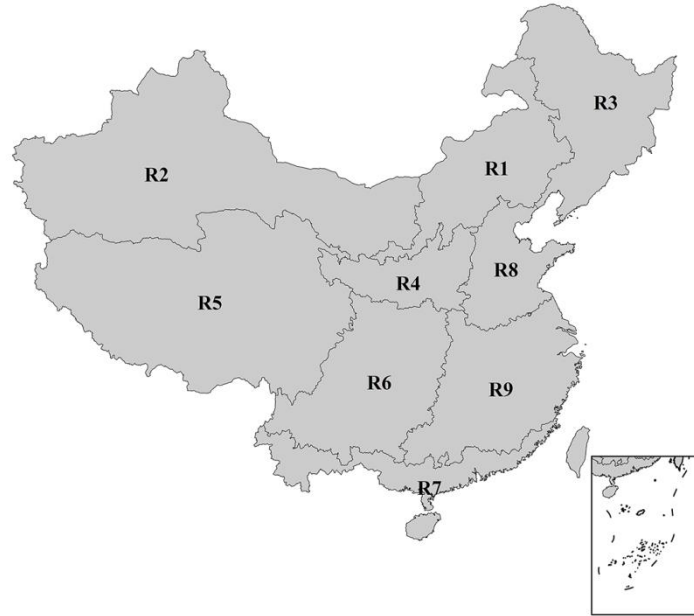


Fig01. The forest cover map of China

1246
 1247
 1248
 1249
 1250
 1251
 1252
 1253
 1254
 1255
 1256
 1257
 1258
 1259
 1260
 1261
 1262
 1263
 1264
 1265
 1266
 1267



1268

1269

Fig02. Map showing the nine regions of China used for detailed analysis

1270

1271

1272

1273

1274

1275

1276

1277

1278

1279

1280

1281

1282

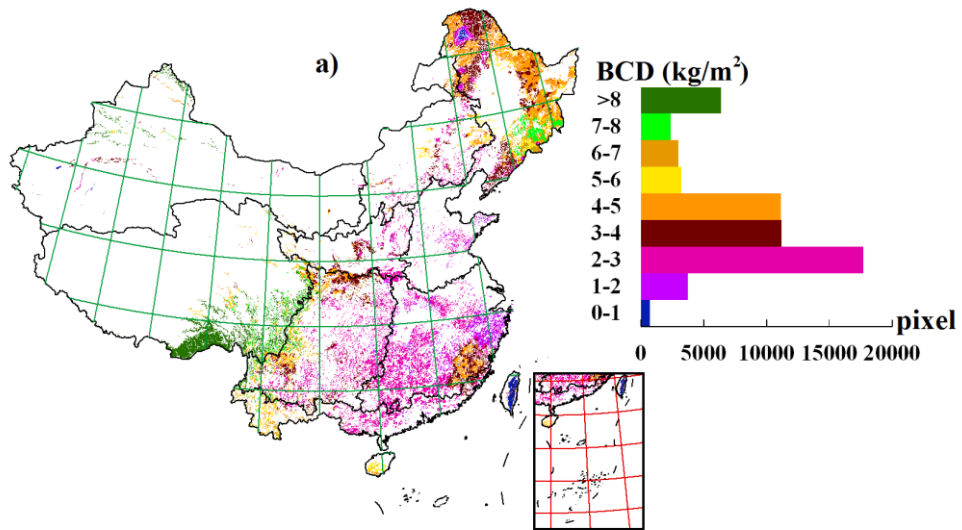
1283

1284

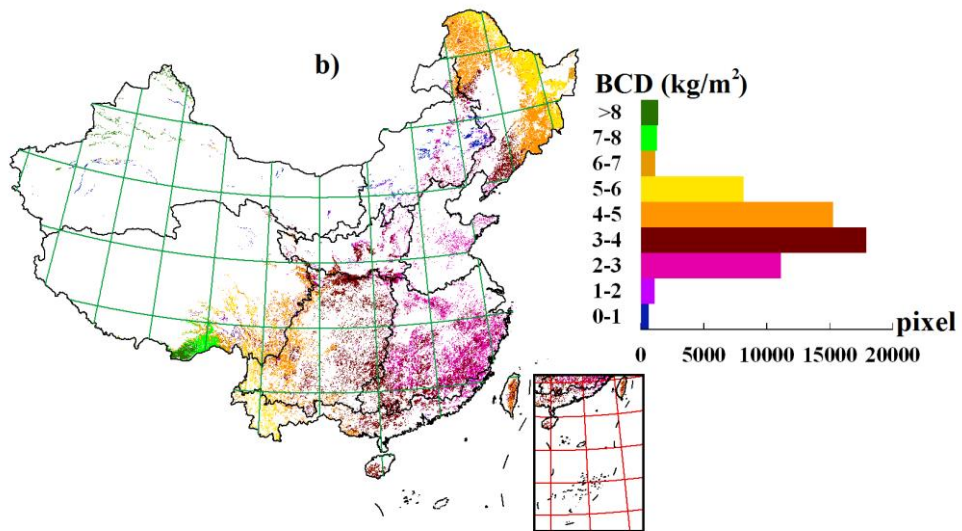
1285

1286

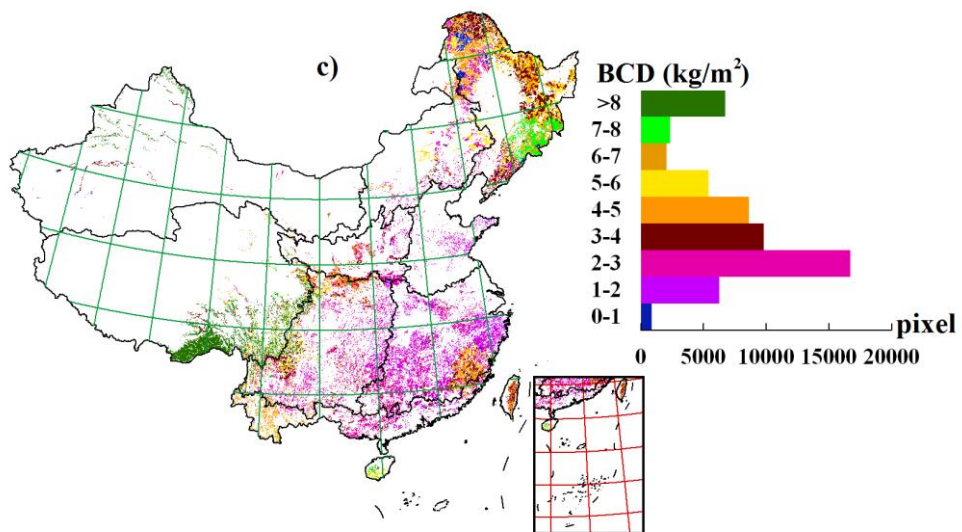
1287



1288



1289



1290

1291

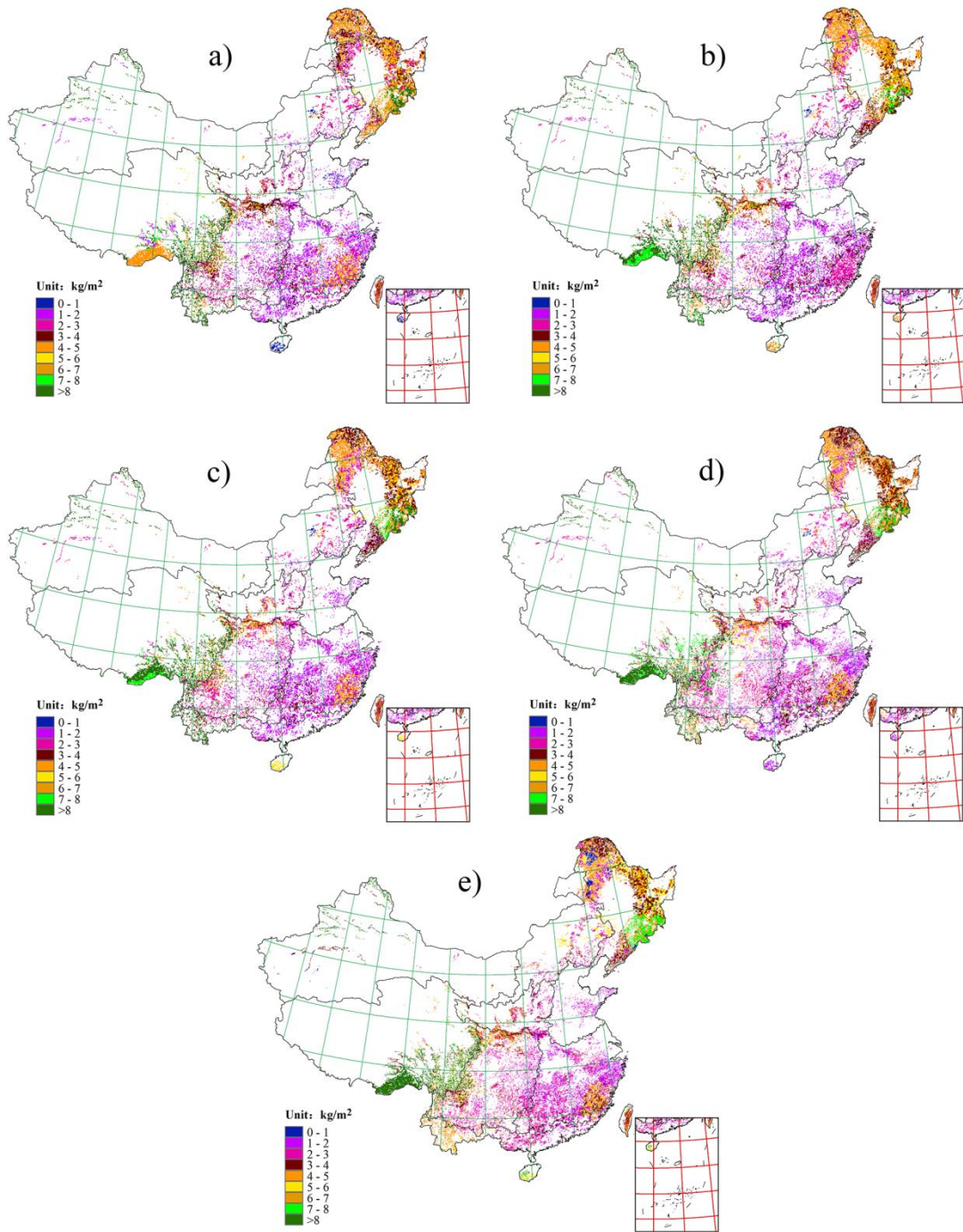
Fig03. The spatial distribution of forest biomass BCDs estimated during the period 2004-2008 in China

1292

using: (a) Kriging; (b) SOA; and (c) HASM-S

1293

1294



1295

1296 **Fig04. The spatial distribution of forest BCDs in China estimated during the five periods using HASM-SOA:**

1297 (a) 1984-1988 (P1); (b) 1989-1993 (P2); (c) 1994-1998 (P3); (d) 1999-2003 (P4); and (e) 2004-2008

1298 (P5)

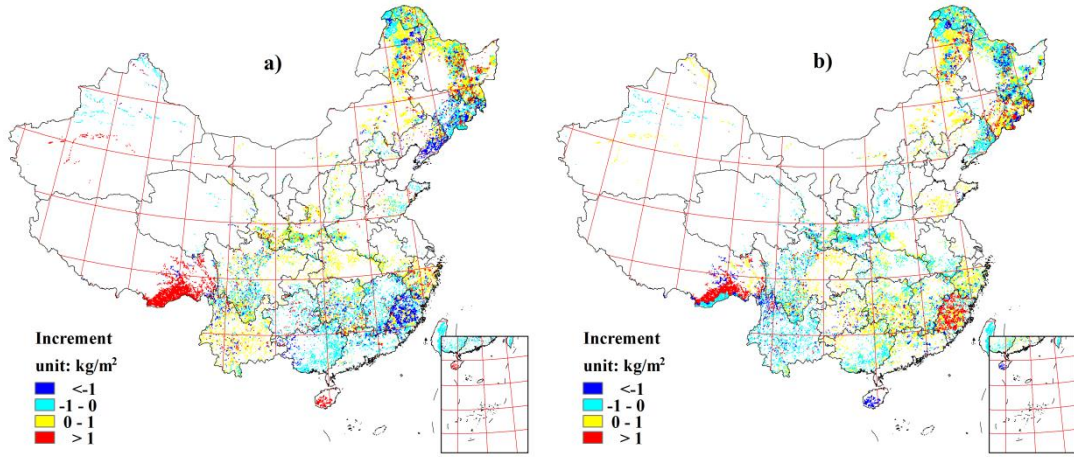
1299

1300

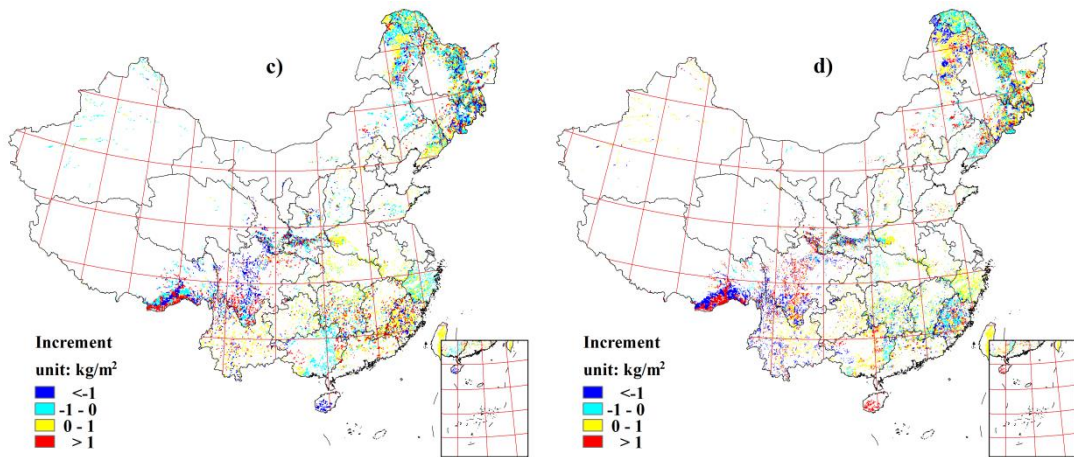
1301

1302

1303



1304



1305

1306

1307

1308

1309

1310

1311

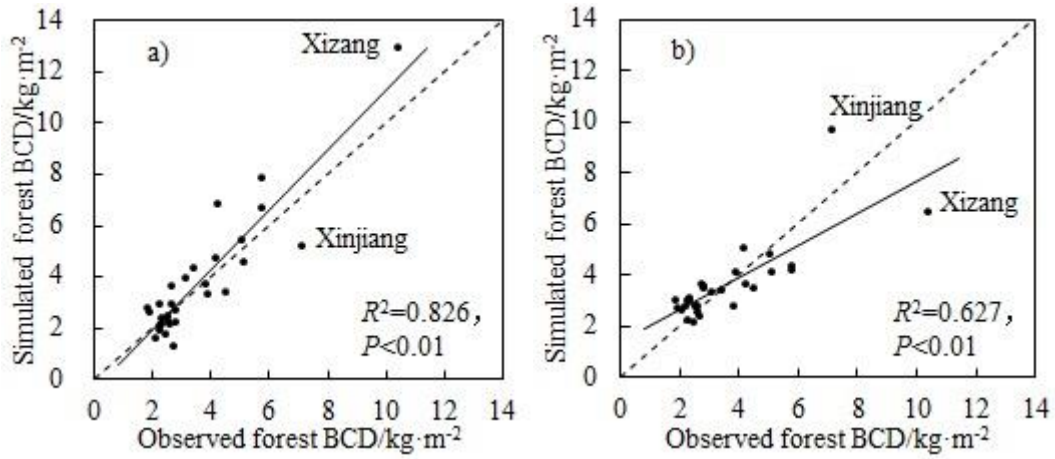
1312

1313

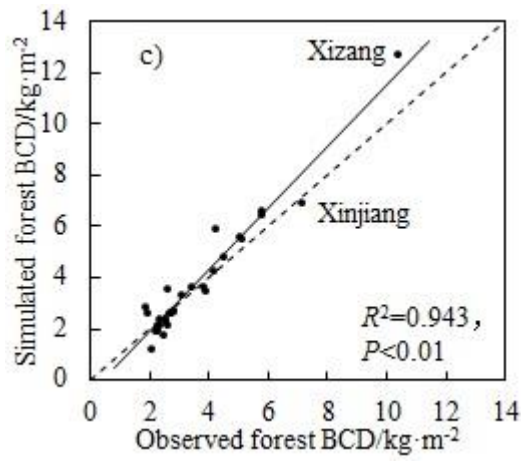
1314

Fig05. The increment maps of biomass carbon stocks from comparing two adjacent periods : a) BCS in Period 2 minus BCS in Period 1, b) BCS in Period 3 minus BCS in Period 2, c) BCS in Period 4 minus BCS in Period 3, and d) BCS in Period 5 minus BCS in Period 4

1315



1316



1317

1318 **Fig06. The scatter diagrams of simulated BCD against observed BCD: a) Kriging, b) SOA, and c)**

1319

HASM-SOA

1320

1321

1322

1323

1324

1325

1326

1327

1328

1329 **List of Abbreviations**

1330

1331	BCD	Biomass Carbon Density
1332	BCS	Biomass Carbon Stock
1333	BEF	Biomass Expansion Factor (method)
1334	CBM	Continuous BEF Method
1335	CF	Carbon Factor
1336	EOS	Earth Observation System
1337	FA	Forest Area
1338	FID	Forestry Inventory Database
1339	HASM	High Accuracy Surface Modeling (method)
1340	MAE	Mean Absolute Error
1341	MBCD	Mean Biomass Carbon Density
1342	MBD	Mean Biomass Density
1343	MRE	Mean Relative Error
1344	MODIS	Moderate-Resolution Imaging System
1345	MR	Mean Ratio
1346	NDVI	Normalized Difference Vegetation Index
1347	NPP	Net Primary Productivity
1348	SOA	Satellite-Observation-based Approach

1349